Superconducting phase qubit based on the Josephson oscillator with strong anharmonicity

A. B. Zorin[1] and F. Chiarello[2]
[1]*Physikalisch-Technische Bundesanstalt, Bundesallee 100, D-38116 Braunschweig, Germany*
[2]*Istituto di Fotonica e Nanotecnologie, CNR, via Cineto Romano 42, I-00156 Rome, Italy*
(Received 27 August 2009; revised manuscript received 19 November 2009; published 30 December 2009)

We propose a superconducting phase qubit on the basis of the radio-frequency superconducting quantum interference device with the screening parameter value $\beta_L \equiv (2\pi/\Phi_0)LI_c \approx 1$, biased by a half-flux quantum $\Phi_e = \Phi_0/2$. Significant anharmonicity (>30%) can be achieved in this system due to the interplay of the cosine Josephson potential and the parabolic magnetic energy potential that ultimately leads to the quartic polynomial shape of the well. The two lowest eigenstates in this global minimum perfectly suit for the qubit which is insensitive to the charge variable, biased in the optimal point and allows an efficient dispersive readout. Moreover, the transition frequency in this qubit can be tuned within an appreciable range allowing variable qubit-qubit coupling.

DOI: 10.1103/PhysRevB.80.214535 PACS number(s): 03.67.Lx, 74.50.+r, 85.25.Dq, 03.67.Pp

The superconducting qubits based on the Josephson tunnel junctions (see, e.g., the reviews in Refs. 1 and 2) have already demonstrated their great potential for the quantum computation.[3] Depending on their design and principle of exploiting the junction nonlinearity, the superconducting qubits are usually classified[2,3] into the categories of charge,[4] charge-phase,[5,6] transmon,[7] flux,[8,9] and phase qubits[10] (roughly in the order of increasing the junction size). The proposed, in this paper, circuit falls into the class of phase qubits, i.e., the devices which are based on energy quantization inside the anharmonic energy wells. Due to rather low electrodynamic impedance these qubits are particularly suitable for integration with microwave on-chip transmission lines and resonators, i.e., the elements which significantly extend the scope of the circuit designs. Moreover, this property of the phase qubits may be particularly advantageous in realization of more complex integrated circuits with quantum behavior.[11] The quantum state tomography[12] and generation of Fock states[13] have been recently demonstrated in the circuits including the phase qubits. Therefore, possible improvement of the phase qubits could have impact on further successful development of solid-state quantum information circuits.

The energy wells of the phase qubits are engineered with the help of nonlinear Josephson inductance whereas self-capacitance of the Josephson junction (JJ) adds a kinetic energy to this oscillatorlike electrical circuit. In the conventional phase qubits, the energy wells are formed by the inclined cosine Josephson potential.[10] Their shape is controlled either by finite bias current with the values slightly below the critical current of the Josephson junction I_c or by finite flux bias Φ_e applied to the qubit loop of sufficiently large inductance.[14] The former case corresponds to the so-called washboard Josephson potential, whereas in the latter case the periodic Josephson potential is superimposed on parabolic magnetic potential forming asymmetric side wells. In both cases, the qubit well can be approximated by the cubic parabola with a smooth energy barrier isolating the shallow well from one side and allowing escape out of this well from another side that enables a simple readout.

The low depth of the cubic parabola well leads to anharmonicity, viz., successive reduction in the transition energies $\Delta E_n = E_{n+1} - E_n$, $n = 0, 1, \ldots$, from bottom to top, necessary for the qubit operation within the basis states $|n=0\rangle$ and $|n=1\rangle$, excluding unwanted excitation of the higher energy states ($n > 1$). Usually the phase qubit is designed such that for appropriate phase bias the cubic potential well includes three-four energy levels with anharmonicity of a few percent.[2,15] This is achieved by adjusting the plasma frequency of the Josephson junction both by designing appropriate parameters of the junction and, possibly, by applying external capacitor shunting. The lowering of the energy barrier by applying the so-called measuring pulse, makes possible the reduction in the number of the levels to two ($n=0$ and 1), with notably different rates of escape to a running-phase state (in the case of current bias), or to the lower-energy state in the adjacent deeper well (in the case of the loop configuration of the qubit). The large (but finite) difference of these tunneling rates sets the maximum theoretical value for the fidelity of such measurement to 96.6%. In the carefully designed and optimally biased qubit the best experimental fidelity values approach 90%.[16] The main disadvantage of such phase qubit is the necessity of resetting it after each measurement.

In contrast to the charge,[4] charge-phase,[5] flux,[8,9] transmon[7] and recently proposed, the so-called fluxonium[17] qubits, the conventional phase qubits cannot inherently operate in an optimal point, i.e., in the symmetric working point insensitive in the first order to the noise that could give drastic improvement to the qubit performance.[5,18] [The exceptions are the recently proposed three-junction interferometer circuit[19] and the so-called camelback potential phase qubit based on the two-junction superconducting quantum interference device (SQUID).[20]] Moreover, the limited anharmonicity of the phase qubit makes the observable reactance impedance (i.e., the Josephson inductance) values in the ground and exited states hardly distinguishable. This poses serious problems for dispersive readout schemes, which proved advantageous where applicable[6,18,21] and have allowed quantum nondemolition measurements as well as high-fidelity measurements based on bifurcation amplifiers.[22,23]

In this paper we propose an improved phase qubit which in contrast to conventional phase qubits is based on a symmetric well possessing significant anharmonicity. Moreover,

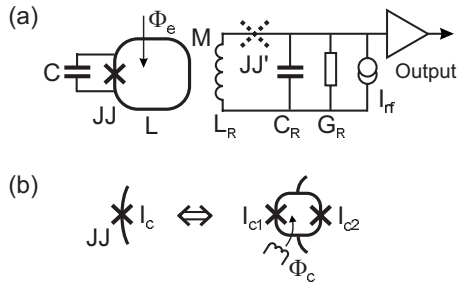

FIG. 1. (a) Electric diagram of the qubit coupled to a resonant circuit and (b) possible equivalent compound (two-junction SQUID) circuit of the Josephson element included into the qubit loop. Capacitance C includes both the self-capacitance of the junction and the external capacitance. Due to inclusion in the resonant circuit of a Josephson junction JJ′, the resonator may operate in the nonlinear regime, enabling a bifurcation-based readout.

the manipulation and dispersive readout of this qubit are both possible in a symmetry point that potentially improves its coherent characteristics. The circuit diagram of our qubit is shown in Fig. 1(a). It comprises the superconducting loop with geometrical inductance L closed by a Josephson junction, generally shunted by an external capacitance, and rf-driven $L_RC_RG_R$ resonance circuit inductively coupled to the qubit loop. The peculiarity of this qubit is the unity value of the SQUID screening parameter $\beta_L \equiv (2\pi/\Phi_0)LI_c \approx 1$, where $\Phi_0 = h/2e$ is the flux quantum. This can be achieved by an accurate design of the circuit including replacement of the single junction with a two-junction SQUID with small loop inductance, allowing more precise adjustment of the resulting critical current I_c [see Fig. 1(b)]. This yields

$$\beta_L(\Phi_c) = (4\pi/\Phi_0)LI_{c0}\cos(\pi\Phi_c/\Phi_0), \tag{1}$$

where I_{c0} is critical current of either Josephson junction and Φ_c is the control flux $(0 \leq \Phi_c < \Phi_0/2)$.

The potential energy of the stand-alone qubit biased by external magnetic flux Φ_e includes the magnetic and Josephson components and can be written as

$$U(\phi, \phi_e) = E_L[0.5(\phi - \phi_e)^2 - \beta_L(1 + \cos\phi)], \tag{2}$$

where $E_L = (\Phi_0/2\pi)^2/L = E_J/\beta_L$ is characteristic magnetic energy associated with the loop inductance, the Josephson coupling energy $E_J = (\Phi_0/2\pi)I_c$, the phase variable ϕ and the phase bias $\phi_e = 2\pi\Phi_e/\Phi_0$. For small values of $\beta_L \ll 1$, the potential Eq. (2) yields the almost parabolic shape of the global single well [first term in Eq. (2)], whereas for the values β_L appreciably greater that 1, the series of wells are superimposed on the global parabola, so the bottom parts of these local minima can also be approximated by the quadratic parabolas. In the case of large density of the levels within these parabolas, the energy spectrum is also close to that of a harmonic oscillator. So, neither of these cases allows significant anharmonicity necessary for the efficient qubit operation.

The essentially different shape of the potential Eq. (2) with $\phi_e = \pi$ is, however, achieved for $\beta_L \approx 1$, i.e., when the quadratic magnetic term is partially compensated by the quadratic term in the Josephson energy expansion near the bottom $(U=0)$ of the single well centered at $\varphi \equiv \phi - \pi = 0$, i.e.,

$$U(\varphi) \approx E_J\left[-\frac{(\beta_L - 1)}{2\beta_L}\varphi^2 + \frac{1}{24}\varphi^4 + O(\varphi^6)\right]. \tag{3}$$

In the ultimate case of $\beta_L = 1$, Eq. (3) provides the obtuse shape of the quartic parabola. Taking into account the finite kinetic energy of the system in corresponding Schrödinger equation, $\hat{Q}^2/2C = -4E_c\partial_{\phi\phi}$, where $\hat{Q} = -i(2e)\partial_\phi$ is the charge operator,[27] one can perform quantization of the system. Application of the quasiclassical quantization rule of Bohr-Sommerfeld yields for this quartic oscillator the energy levels obeying the 4/3 power law[28]

$$E_n^{(\mathrm{qc})} = \epsilon(n + 1/2)^{4/3} \tag{4}$$

with prefactor ϵ which in terms of the parameters of our circuit is equal to

$$\epsilon = 2^{-5/3}3[\pi/K(1/2)]^{4/3}(E_JE_c^2)^{1/3} \approx 1.9(E_JE_c^2)^{1/3}, \tag{5}$$

where $K(k)$ is the complete elliptic integral of the first kind. Thus, the energy spectrum in the quartic potential takes intermediate position between the equidistant spectrum of the harmonic oscillator $E_n \propto (n+1/2)$ and that of the rectangular well, $E_n \propto (n+1)^2$, having extremely high anharmonicity. Expressions (4) and (5) are exact for the higher levels $(n \gg 1)$ and large "mass" (capacitance C), ensuring the very large ratio of the Josephson energy E_J to the charging energy $E_c = e^2/2C$. An estimate of the anharmonicity factor in this quasiclassical approximation can be immediately obtained from Eq. (4)

$$\delta_{\mathrm{qc}} = (\Delta E_1 - \Delta E_0)/\Delta E_0 \approx 26\%. \tag{6}$$

The numerical solution of the corresponding Schrödinger equation with potential energy Eq. (2) yields in the limit $E_J/E_c \gg 1$ an even larger value of the anharmonicity factor, $\delta \approx 33\%$ (see the energy spectrum in Fig. 2). These values substantially exceed the typical anharmonicity values of the conventional phase qubit, $|\delta_{\mathrm{phase}}| \approx 3\%$, for the number of levels inside the cubic-parabola well equal to four,[2,15] and transmon qubit, $|\delta_{\mathrm{transmon}}| \approx (E_c/8E_J)^{1/2} \lesssim 5\%$ for optimum values $E_J/E_c \gtrsim 50$.[7] Moreover, in contrast to the negative values of δ in these examples, the series of the energy levels in the quartic potential has positive value $\delta > 0$, i.e., corresponds to successively increasing level spacings $\Delta E_1 < \Delta E_2 < \Delta E_3 < \cdots$.

Such a large, positive anharmonicity is a great advantage of the quartic potential qubit allowing manipulation within the two basis qubit states $|0\rangle$ and $|1\rangle$ not only when applying resonant microwave field, $\nu_{\mu\mathrm{w}} \approx \nu_{10}$ but also when applying control microwave signals with large frequency detuning or using rather wide-spectrum rectangular-pulse control signals. The characteristic qubit frequency $\nu_{10} = \Delta E_0/h$ and the anharmonicity factor δ computed from the Schrödinger equation for the original potential Eq. (2) in the range $0.9 \leq \beta_L \leq 1.02$ are shown in Fig. 3. One can see that the significant range in the tuning of the qubit frequency within the range of sufficiently large anharmonicity (~20–50 %) is attained at a

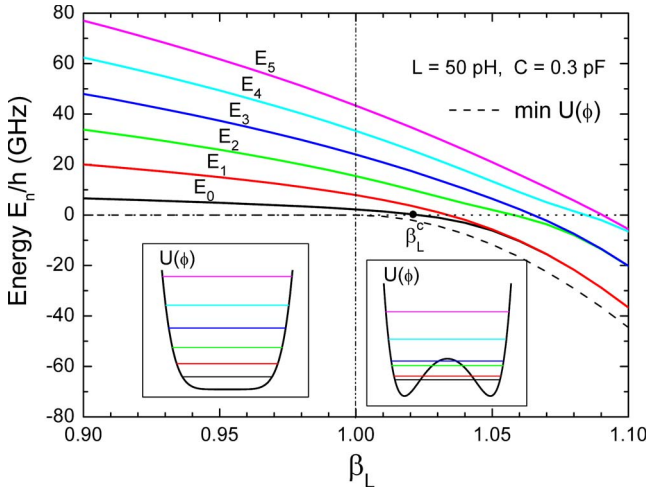

FIG. 2. (Color online) Position of the lowest six levels (solid lines) in the potential Eq. (2) for $\phi_e=\pi$ as a function of parameter $\beta_L \propto I_c$ [in experiment, controlled by external magnetic flux Φ_c, see Eq. (1)] for typical values of L and C yielding $E_J/E_c \sim E_L/E_c \approx 5.1\times 10^4$. With an increase in β_L, the spectrum crosses over from that of the harmonic oscillator type (left inset) to the set of the doublets (right inset), corresponding to the weak coupling of the oscillator-type states in two separate wells (the flux qubit limit). The spectrum in the central region $\beta_L \approx 1$ is strongly anharmonic. The dashed line shows the bottom energy of the potential $U(\phi, \phi_e=\pi)$, which in the case of $\beta_L>1$ is equal to $-\Delta U \approx -1.5E_L(\beta_L-1)^2/\beta_L$ (in other words, ΔU is the height of the energy barrier in the right inset) (Refs. 24 and 25). The dotted (zero-level) line indicates the energy in the symmetry point $\phi=0$, i.e., at the bottom of the single well ($\beta_L \leq 1$) or at the top of the energy barrier ($\beta_L>1$). The black dot shows the critical value β_L^c at which the ground-state energy level touches the top of the barrier separating the two wells.

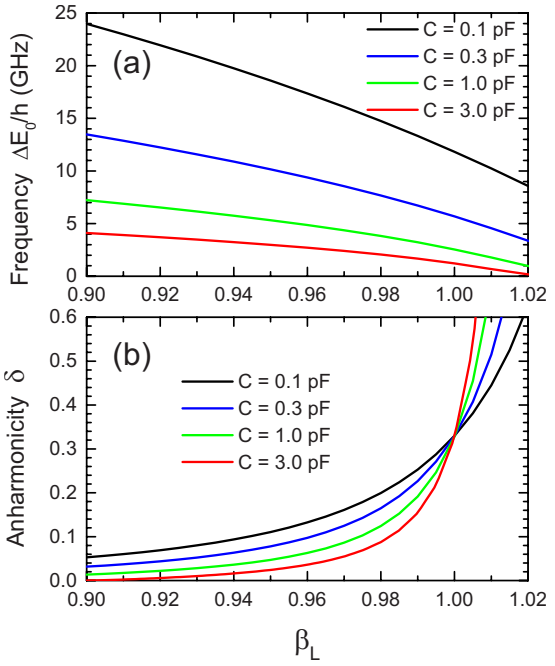

FIG. 3. (Color online) (a) The qubit frequency as a function of parameter β_L for fixed $L=50$ pH and several values of capacitance $C=0.1$, 0.3, 1.0, and 3.0 pF (from top to bottom), corresponding to the values of the ratio $E_L/E_c \approx 1.7\times 10^4$, 5.1×10^4, 1.7×10^5, and 5.1×10^5. (b) Anharmonicity parameter δ as a function of parameter β_L for the same as in (a) inductance L and capacitance values (from top to bottom).

rather fine (typically $\pm 1-2$ %) tuning of β_L around the value $\beta_L=1$. Such tuning of β_L is possible in the circuit having the compound configuration shown in Fig. 1(b). For values of $\beta_L>1$, the symmetric energy potential has two minima and a barrier between them. The position of the ground-state level depends on β_L and the ratio of the characteristic energies $E_J/E_c=\beta_L E_L/E_c$. The value of β_L at which the ground-state level touches the top of the barrier sets the upper limit β_L^c for the quartic qubit (marked in Fig. 2 by solid dot). At $\beta_L>\beta_L^c$, the qubit energy dramatically decreases and the qubit states are nearly the symmetric and antisymmetric combinations of the states inside the two wells (see the right inset in Fig. 2 showing this flux-qubit limit). Although the qubit with such parameters has very large anharmonicity and can be nicely controlled by dc flux pulses,[25,26] its readout can hardly be accomplished in a dispersive fashion, because very large E_J/E_c yields in our case exponentially small splitting of the qubit levels. These levels are extremely critical to the symmetry of the energy potential. So even small amplitude of radio-frequency readout signal will significantly tilt the qubit potential and therefore ruin the basis levels.

Another advantage of the phase qubit having the energy potential of the shape close to the quartic one is a strong dependence of its Josephson inductance $L_J(\Phi_e,n)$ on the quantum state $|n\rangle$. The observed value of the reverse inductance is related to the local curvature of the dependence of corresponding energy E_n on flux Φ_e (see, e.g., Ref. 18),

$$L_J^{-1}(\Phi_e,n)=\frac{2\pi}{\Phi_0}\langle n|\frac{\partial \hat{I}(\phi,\phi_e)}{\partial \phi_e}|n\rangle=\frac{\partial^2 E_n(\Phi_e)}{\partial \Phi_e^2}, \qquad (7)$$

where $\hat{I}$ is the operator of supercurrent circulating in the qubit loop. The dependence of the reverse inductance $L_J(\Phi_e=\Phi_0/2,n)$ calculated numerically in the two lowest quantum states ($n=0$ and 1) for $L=50$ pH and the same set of capacitances C as in Fig. 3 is shown in Fig. 4. One can see that the ratio of the geometrical to Josephson inductances L/L_J takes large and very different values that can be favorably used for the dispersive readout, ensuring a sufficiently large output signal. Note that for $\beta_L<1$, both inductances $L_J(n=0)$ and $L_J(n=1)$ are negative, whereas at $\beta_L>1$ the inductance $L_J(n=1)$ changes the sign to positive.

The readout of this qubit is based on the measurements of the reactive part (inductance) of the loop impedance probed by a low-frequency ac signal, $f \ll \nu_{10}$ of sufficiently small amplitude[29] (see also Ref. 6). This signal is supplied by a rf-driven oscillator [Fig. 1(a)] as an alternating biasing flux, $\Phi_e=0.5\Phi_0+MI_L$ or $\phi_e=\pi+\delta\phi_e$, where $\delta\phi_e=a\cos(2\pi ft)$ with $a \ll 1$. Here $M=\kappa(LL_R)^{1/2}$ is mutual inductance, κ, a dimensionless coupling coefficient and I_L, the current in inductance L_R. Coupling of the qubit to the resonance tank circuit causes renormalization of the circuit inductance (see, e.g., Refs. 6 and 18),

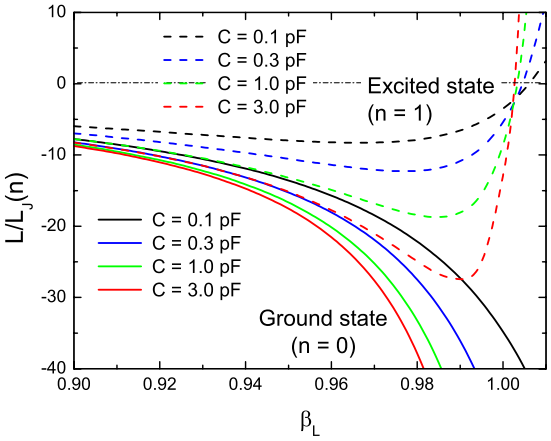

FIG. 4. (Color online) The values of the Josephson inductance of the quartic potential qubit in the ground (solid lines) and excited (dashed lines) states calculated for the geometric inductance value $L=50$ pH and the set of capacitances C, increasing from top to bottom for both groups of curves.

$$L_R^{(n)} = L_R[1 - \kappa^2 L/L_J(n)], \tag{8}$$

and the resonance frequencies $\omega_n=[L_R^{(n)}C]^{-1/2}$, where $n=0$ and 1. The relative difference of the resonance frequencies for the qubit in the excited and ground states is

$$\frac{\delta\omega}{\omega_0} = \frac{\omega_1 - \omega_0}{\omega_0} = \sqrt{\frac{1 - \kappa^2 L/L_J(0)}{1 - \kappa^2 L/L_J(1)}} - 1. \tag{9}$$

Figure 5 shows this relative frequency shift versus parameter β_L. One can see that for the rather conservative value of dimensionless coupling $\kappa=0.05$, the relative frequency shift can achieve the easily measured values of about 10%. The efficiency of the dispersive readout can be improved in the nonlinear regime with bifurcation.[22] With our device this regime can be achieved in the resonance circuit including, for example, a Josephson junction (marked in the diagram in Fig. 1 by a dashed cross). Due to the high sensitivity of the amplitude (phase) bifurcation to the threshold determined by the effective resonance frequency of the circuit, one can expect a readout with high fidelity even at a rather weak coupling of the qubit and the resonator (compare with the readout of quantronium in Ref. 30). Further improvement of the readout, including good control of the circuit parameters, can be achieved applying the cavity bifurcation amplifier.[31]

The loop configuration and frequency detuning of the quartic qubits should allow their inductive coupling with variable strength keeping both qubits in optimal points. Variable coupling of the optimally biased qubit to a superconducting resonator is also possible. More sophisticated coupling of the pairs of quartic qubits can be accomplished, for example, using a Josephson-junction coupler in a fashion recently proposed by Harris *et al.*[32]

In conclusion, we have shown that the phase qubit of the rf-SQUID configuration with parameter $\beta_L \approx 1$ and flux bias $\Phi_e=\Phi_0/2$ has remarkable characteristics. It can be easily integrated into available technology and allow controllable

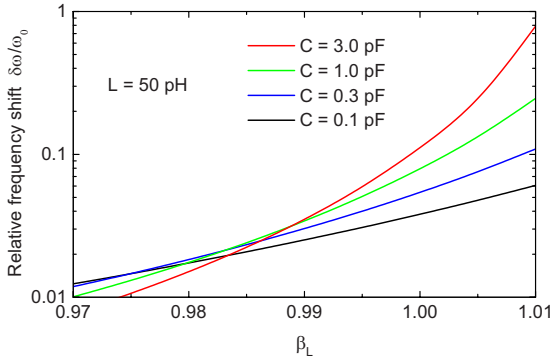

FIG. 5. (Color online) The resonance frequency shift in the circuit due to excitation of the qubit with the inductance value $L=50$ pH and the set of capacitances C, decreasing from top to bottom. The dimensionless coupling coefficient $\kappa=0.05$.

coupling to qubits and electrical and mechanical resonators. Still, we expect that implementation of this qubit requires the solution of several experimental problems. For example, due to a high sensitivity of the qubit parameters to the magnitude of β_L, whose optimum values lie within a rather narrow range ($\pm 1-2$ %), particular precaution should be taken against fluctuations in the line controlling the effective Josephson coupling in the circuit [see Fig. 1(b)], because otherwise it may cause significant dephasing of the qubit. Furthermore, flux bias $\Phi_e=\Phi_0/2$ should also be set as precisely as possible. Experimentally, it can be realized either by freezing the flux $\Phi_e=\Phi_0$ in the main loop having a symmetric gradiometer configuration,[33] or by including in the loop of a Josephson π junction[34] with a sufficiently high critical current ensuring the steady phase shift of π.

Another advantage of the proposed quartic qubit, which is particularly important for scalable circuits, is that the readout of these qubits can be performed without resetting them. In contrast to conventional phase qubits, the basis states of the quartic qubits are associated with a global minimum and their (dispersive) readout never causes escape out of this minimum. Such escape is usually followed by sequential quantum transitions (relaxation) inside the adjacent (deeper) well. This relaxation in an adjacent idle well causes, first, unavoidable delay in the circuit operation and, second, generation of microwave-frequency photons which may present a problem in integrated systems because of possible interaction with the rest of the circuit.[35]

Of course, similar to properties of the conventional types of the phase qubits, the coherence characteristics of the quartic qubit will be strongly dependent on the material properties of the circuit. Minimizing the losses due to the qubit coupling to microscopic degrees of freedom (two-level systems) inside the dielectrics surrounding the superconducting circuit (the substrate, insulator inside the capacitor, the junction barriers, etc.) play crucial role for improving the qubit coherence.[11] Since the operation and tuning of the quartic qubit is possible without leaving the optimal point, one may expect a weaker coupling of the qubit to these microscopic two-level systems located inside dielectrics and, therefore, a better quantum coherence. Moreover, the zero persistent supercurrent circulating in the qubit loop of the qubit with

single junction at the optimum bias, $\phi_e = \pi$, may also reduce the effect of quasiparticle tunneling on the qubit coherence. Probably, such weakening of the qubit coupling to external degrees of freedom can explain reasonably good coherence characteristics ($\tau_{\mathrm{Rabi}} \approx 60$ ns) of the Nb camelback qubit operated in an optimal point at zero persistent current.[20] Anyway, the properties of the proposed quartic qubit will be clarified in experiment which is currently in the preparation stage.

We thank Michael Wulf and Ralf Dolata for useful discussions. This work was partially supported by the EU through the EuroSQIP project and DFG (German Science Foundation) through Grant No. ZO124/2-1.

[1] Yu. Makhlin, G. Schön, and A. Shnirman, Rev. Mod. Phys. **73**, 357 (2001).
[2] M. H. Devoret and J. M. Martinis, Quantum Inf. Process. **3**, 163 (2004).
[3] G. Wendin and V. S. Shumeiko, in *Handbook of Theoretical and Computational Nanotechnology*, edited by M. Rieth and W. Schommers (ASP, Los Angeles, 2006), Vol. 3, p. 223.
[4] Y. Nakamura, Yu. A. Pashkin, and J. S. Tsai, Nature (London) **398**, 786 (1999).
[5] D. Vion, A. Aassime, A. Cottet, P. Joyez, H. Pothier, C. Urbina, D. Esteve, and M. H. Devoret, Science **296**, 886 (2002).
[6] A. B. Zorin, Physica C **368**, 284 (2002).
[7] J. Koch, T. M. Yu, J. Gambetta, A. A. Houck, D. I. Schuster, J. Majer, A. Blais, M. H. Devoret, S. M. Girvin, and R. J. Schoelkopf, Phys. Rev. A **76**, 042319 (2007).
[8] J. R. Friedman, V. Patel, W. Chen, S. K. Tolpygo, and J. E. Lukens, Nature (London) **406**, 43 (2000).
[9] I. Chiorescu, Y. Nakamura, C. J. P. M. Harmans, and J. E. Mooij, Science **299**, 1869 (2003).
[10] J. M. Martinis, S. Nam, J. Aumentado, and C. Urbina, Phys. Rev. Lett. **89**, 117901 (2002).
[11] J. M. Martinis, Quantum Inf. Process. **8**, 81 (2009).
[12] M. Steffen, M. Ansmann, R. C. Bialczak, N. Katz, E. Lucero, R. McDermott, M. Neeley, E. M. Weig, A. N. Cleland, and J. M. Martinis, Science **313**, 1423 (2006).
[13] M. Hofheinz, E. M. Weig, M. Ansmann, R. C. Bialczak, E. Lucero, M. Neeley, A. D. O'Connell, H. Wang, J. M. Martinis, and A. N. Cleland, Nature (London) **454**, 310 (2008).
[14] R. W. Simmonds, K. M. Lang, D. A. Hite, S. Nam, D. P. Pappas, and J. M. Martinis, Phys. Rev. Lett. **93**, 077003 (2004).
[15] M. Steffen, J. M. Martinis, and I. L. Chuang, Phys. Rev. B **68**, 224518 (2003).
[16] E. Lucero, M. Hofheinz, M. Ansmann, R. C. Bialczak, N. Katz, M. Neeley, A. D. O'Connell, H. Wang, A. N. Cleland, and J. M. Martinis, Phys. Rev. Lett. **100**, 247001 (2008).
[17] V. E. Manucharyan, J. Koch, L. I. Glazman, and M. H. Devoret, Science **326**, 113 (2009).
[18] A. B. Zorin, JETP **98**, 1250 (2004).
[19] F. Chiarello, M. G. Castellano, G. Torrioli, S. Poletto, C. Cosmelli, P. Carelli, D. V. Balashov, M. I. Khabipov, and A. B. Zorin, Appl. Phys. Lett. **93**, 042504 (2008).
[20] E. Hoskinson, F. Lecocq, N. Didier, A. Fay, F. W. J. Hekking, W. Guichard, O. Buisson, R. Dolata, B. Mackrodt, and A. B. Zorin, Phys. Rev. Lett. **102**, 097004 (2009).
[21] A. Lupaşcu, C. J. M. Verwijs, R. N. Schouten, C. J. P. M. Harmans, and J. E. Mooij, Phys. Rev. Lett. **93**, 177006 (2004).
[22] I. Siddiqi, R. Vijay, F. Pierre, C. M. Wilson, M. Metcalfe, C. Rigetti, L. Frunzio, and M. H. Devoret, Phys. Rev. Lett. **93**, 207002 (2004).
[23] A. Lupaşcu, E. F. C. Driessen, L. Roschier, C. J. P. M. Harmans, and J. E. Mooij, Phys. Rev. Lett. **96**, 127003 (2006).
[24] F. Chiarello, Phys. Lett. A **277**, 189 (2000).
[25] F. Chiarello, Eur. Phys. J. B **55**, 7 (2007).
[26] S. Poletto, F. Chiarello, M. G. Castellano, J. Lisenfeld, A. Lukashenko, C. Cosmelli, G. Torrioli, P. Carelli, and A. V. Ustinov, New J. Phys. **11**, 013009 (2009).
[27] P. W. Anderson, in *Lectures on Many-Body Problem*, edited by E. R. Caianiello (Academic, New York, 1964), Vol. 2, p. 113.
[28] See, for example, A. M. Sánchez and J. D. Bejarano, J. Phys. A **19**, 887 (1986) and references therein.
[29] R. Rifkin and B. S. Deaver, Jr., Phys. Rev. B **13**, 3894 (1976).
[30] I. Siddiqi, R. Vijay, M. Metcalfe, E. Boaknin, L. Frunzio, R. J. Schoelkopf, and M. H. Devoret, Phys. Rev. B **73**, 054510 (2006).
[31] M. B. Metcalfe, E. Boaknin, V. Manucharyan, R. Vijay, I. Siddiqi, C. Rigetti, L. Frunzio, R. J. Schoelkopf, and M. H. Devoret, Phys. Rev. B **76**, 174516 (2007).
[32] R. Harris, T. Lanting, A. J. Berkley, J. Johansson, M. W. Johnson, P. Bunyk, E. Ladizinsky, N. Ladizinsky, T. Oh, and S. Han, Phys. Rev. B **80**, 052506 (2009).
[33] J. B. Majer, J. R. Butcher, and J. E. Mooij, Appl. Phys. Lett. **80**, 3638 (2002).
[34] L. B. Ioffe, V. B. Geshkenbein, M. V. Feigel'man, A. L. Fauchere, and G. Blatter, Nature (London) **398**, 679 (1999).
[35] J. M. Martinis (private communication).